IEEE Journal of Microwaves

Received 16 August 2022; revised 20 November 2022; accepted 29 November 2022. Date of publication 20 December 2022; date of current version 6 January 2023.

Digital Object Identifier 10.1109/JMW.2022.3227048

Closed-Loop Wireless Power Transfer With Adaptive Waveform and Beamforming: Design, Prototype, and Experiment

SHANPU SHEN (Member, IEEE), JUNGHOON KIM, AND BRUNO CLERCKX (Fellow, IEEE)

(Regular Paper)

Department of Electrical and Electronic Engineering, Imperial College London, London SW7 2AZ, U.K.

CORRESPONDING AUTHOR: Shanpu Shen (e-mail: s.shen@imperial.ac.uk).

This work was supported by EPSRC of U.K. under Grants EP/P003885/1 and EP/R511547/1.

ABSTRACT A closed-loop far-field wireless power transfer (WPT) system with adaptive waveform and beamforming using limited feedback is designed, prototyped, and experimented. Spatial domain and frequency domain are jointly exploited by utilizing waveform and beamforming at the transmitter in WPT system to adapt to the multipath fading channel and boost the output dc power. A closed-loop architecture based on a codebook design and an over-the-air limited feedback with low complexity is proposed. The codebook consists of multiple codewords where each codeword represents particular waveform and beamforming. The transmitter sweeps through the codebook and the receiver then feeds the optimal codeword index back to the transmitter, so that the waveform and beamforming can be adaptive for maximizing the output dc power without requiring explicit channel estimation and the knowledge of accurate Channel State Information. The proposed closed-loop WPT with adaptive waveform and beamforming using limited feedback is prototyped using a Software Defined Radio equipment and measured in two real indoor environments. It is experimentally shown that the proposed closed-loop WPT with adaptive waveform and beamforming is able to enhance the output dc power by up to 14.7 dB in comparison with conventional 1-tone 1-antenna WPT system.

INDEX TERMS Beamforming, closed-loop, limited feedback, waveform, wireless power transfer.

I. INTRODUCTION

Far field wireless power transfer (WPT) through radio-frequency (RF) has gained growing interests as a promising technology for energizing massive low duty-cycle and low-power devices in applications including Internet of Things and Wireless Sensor Networks [1]. Compared with batteries that need to be periodically recharged and replaced, far-field WPT, that uses a rectenna to harvested RF energy from a transmitter, is more controllable and reliable. However, in far-field WPT one challenging issue is to enhance the output dc power level given that the transmit power is fixed.

To solve this issue, the vast majority of the research has focused on designing efficient rectenna. There are various rectenna design techniques for enhancing output dc power, including multiband rectenna [2], [3], [4], [5], multiport rectenna [6], [7], [8], [9], [10], compact rectenna [11], [12], metasurface rectenna [13], [14], tightly coupled array rectenna [15], [16], multiband and broadband rectifier [17], [18], high-efficiency rectifier [19], [20], [21], [22], reconfigurable rectifier [23], and hybrid RF-solar harvester [24], [25].

Designing efficient WPT signals is another and complementary research area for enhancing the output dc power [26], [27]. One promising signal strategy is the waveform. The waveform shape of input signal affects the RF-to-dc efficiency due to the rectifier nonlinearity [28]. Simulations and experiments show that using multi-tone waveforms [29], [30], [31], [32] and other waveforms including chaotic, white noise, and orthogonal frequency division multiplexing (OFDM) [33] are able to enhance the RF-to-dc efficiency. However, there are two limitations in these works [29], [30], [31], [32], [33]. *First*, they ignore that the channel between the transmitter and receiver has multipath fading, though multipath makes

the waveform input into the rectifier at the receiver different from the waveform transmitted by the transmitter. *Second*, they are open-loop WPT systems where the waveforms are non-adaptive and designed without considering any Channel State Information (CSI) of multipath fading channel, which degrades the output dc power. Therefore, a closed-loop WPT system with waveform adaptive to the multipath fading channel is needed [34].

Another effective signal strategy for enhancing the output dc power is using multiple antennas with efficient beamforming at the transmitter. By using beamforming, the RF signal transmitted by each antenna element can be coherently added together and thus the output dc power can be enhanced [35]. Various WPT systems with beamforming have been prototyped including using digital beamforming through baseband precoding [36], time-modulation array [37], [38], and phased array [39]. Particularly, a selective and tracking WPT system using backscattering for feedback has been designed in [36]. Besides, to implement adaptive beamforming, WPT systems utilizing receive signal strength indicator [40], [41], [42] or second/third harmonics [43], [44], [45] for feedback have been designed. However, the limitation of these works [36], [37], [38], [39], [40], [41], [42], [43], [44], [45] is that they only focus on using beamforming but did not consider using efficient waveform design. Therefore, together with the two aforementioned limitations of the WPT waveform designs [29], [30], [31], [32], [33], it is found that closed-loop WPT systems utilizing adaptive waveform as well as beamforming are needed.

A unified and systematic theoretical study of adaptive waveform and beamforming design for closed-loop WPT systems was first conducted in [46], with further notable extensions in [47], [48], [49], [50]. Simulations in those papers demonstrated the significant benefits of a systematic design of adaptive waveform and beamforming. However, results were not demonstrated experimentally. In [51], an experimental WPT system with adaptive waveform only was prototyped and experimented. In [52] and more recently in [53], the first experimental WPT system implementing adaptive waveform and beamforming was prototyped and experimented, and results demonstrated the significant advantages of dc power enhancement and range expansion of a WPT architecture relying on channel-adaptive waveform and beamforming. However, those experimental works used complex channel estimation at the receivers (based on OFDM channel estimation and pilot transmission, reminiscent of communication system) and cable feedback mechanisms that do not lend themselves easily to real-world setup with energy-constrained devices. The limitation of those experimental works is therefore that how to acquire CSI at the transmitter with high energy efficiency and low complexity was not solved. In addition, a WPT system with distributed antennas using channel-adaptive antenna selection and frequency selection has been designed, prototyped, and experimented in [54]. However, antenna selection is less efficient than beamforming and frequency selection is less efficient than multi-tone waveform, which limit the output dc power.

In this paper, the first closed-loop WPT system which implements adaptive waveform and beamforming using over-the-air limited feedback technique is designed, prototyped, and experimented. The contributions are shown below.

First, we propose a closed-loop WPT system architecture that exploits frequency domain, spatial domain, and the rectifier nonlinearity by jointly utilizing multi-tone waveform and multi-antenna beamforming to enhance the output dc power effectively. The architecture uniquely relies on a codebook design and an over-the-air limited feedback technique which has low complexity and utilizes an RF interface under IEEE 802.15.4 standard. The codebook is predefined and consists of multiple codewords where each codeword represents particular waveform and beamforming. During a training phase, the transmitter sweeps through the codebook and the receiver measures the output dc power for each codeword and feeds the optimal codeword index back to the transmitter. Then, the transmitter can transfer power using the optimal waveform and beamforming during a WPT phase. The operation is repeated periodically. With the designed codebook and limited feedback, the channel estimation and accurate CSI can be avoided and more importantly the waveform and beamforming is optimized to adapt to the multipath fading channel in real time.

Second, we design, prototype, and experiment the proposed closed-loop WPT system using limited feedback by leveraging a Software Defined Radio (SDR) equipment. This is the first prototype for the closed-loop WPT system with adaptive waveform and beamforming using over-the-air limited feedback to the authors' best knowledge. We measure the proposed WPT system prototype in two real indoor environments. We also measure a closed-loop WPT system utilizing cable-feedback as well as an open-loop WPT system for comparison. It is experimentally shown that using closed-loop adaptive multi-tone waveform and multi-antenna beamforming can effectively enhance the output dc power. In comparison with conventional 1-tone 1-antenna WPT system, the proposed closed-loop WPT system using limit feedback is able to enhance the output dc power by up to 14.7 dB and significantly increase the end-to-end WPT efficiency defined as the ratio of output dc power and transmit RF power. For example, the end-to-end WPT efficiency can be increased from 4.3×10^{-7} to 1.3×10^{-5} and from 9.7×10^{-6} to 5.8×10^{-5} at some locations. In addition, in comparison with the closed-loop WPT system using cable-feedback, the proposed closed-loop WPT system using limited feedback can achieve similar performance while it is more practical since it does not require knowing the CSI.

Table 1 shows a comparison of this work and related work:

1) Compared with [35], [46], [47], [48], [49], [50] which only have numerical simulation results without any convincing experimental verification, this work considers

TABLE 1. Comparison of This Work and Previous Related Work

Reference	Using adaptive beamforming	Using adaptive waveform	Requiring accurate CSI	Simulation or experiment	Using limited feedback
[29]-[33]	No	No	N.A.	Experiment	N.A.
[35]	Yes	No	Yes	Simulation	No
[36]-[45]	Yes	No	No	Experiment	Yes
[46]-[48]	Yes	Yes	Yes	Simulation	No
[49]	Yes	Yes	No	Simulation	Yes
[50]	Yes	Yes	Yes	Simulation	No
[51]	No	Yes	Yes	Experiment	No
[52]-[53]	Yes	Yes	Yes	Experiment	No
[54]	No	No	No	Experiment	Yes
This work	Yes	Yes	No	Experiment	Yes

designing and prototyping a closed-loop WPT system and experimentally verifies the benefit of adaptive waveform and beamforming using over-the-air limited feedback. Particularly, for the limited feedback technique in [49], the limitations are that it does not provide a flow chart to show how the transmitter and receiver cooperate with each other to implement the limited feedback and that it only evaluates the limited feedback technique using an ideal Rayleigh fading channel without channels in real environment. For the waveform and beamforming technique in [50], the limitation is that it requires accurate CSI using channel estimation based on pilot transmission, which increases energy consumption and complexity.

2) Compared with [29], [30], [31], [32], [33] which only consider open-loop waveform design and [36], [37], [38], [39], [40], [41], [42], [43], [44], [45] which only consider beamforming design, this work considers both waveform and beamforming designs which has a higher output dc power.
3) Compared with [51], [52], [53] which require accurate CSI using channel estimation with pilot transmission and coaxial cable feedback, this work uses the over-the-air limited feedback to avoid requiring accurate CSI, which is energy-efficient, low-complexity, and practical for real-world setup.
4) Compared with [54] which uses frequency and antenna selections, this work uses adaptive waveform and beamforming which provides higher output dc power.

To conclude, compared with related work which only has numerical simulation or overlook practical issues such as channel condition [49], flow chart design for transmitter and receiver [49], and CSI acquisition [50], this work has substantial innovation and strength that we design, prototype, and experiment the first closed-loop WPT system with adaptive waveform and beamforming using over-the-air limited feedback, which greatly enhances the output dc power while avoiding power-consuming and complex channel estimation to acquire accurate CSI. To the authors' best knowledge, it is the first work demonstrating experimentally the feasibility and benefits of a closed-loop WPT architecture with adaptive waveform and beamforming based on limited feedback.

Organization: The model and design for the closed-loop WPT system using limited feedback are provided in Sections II and III respectively. The experimental results are shown in Section IV. Conclusions are made in Section V.

Notations: Symbols not in bold font denote scalars. Bold lower letters denote vectors. $|x|$ and $\Re\{x\}$ respectively denote the modulus and real part of a complex scalar x. $\mathbf{x}^T$, $\mathbf{x}^H$, and $\|\mathbf{x}\|$ respectively denote the transpose, conjugate transpose, and l_2-norm of a vector $\mathbf{x}$.

II. CLOSED-LOOP WIRELESS POWER TRANSFER

A. SYSTEM MODEL

Consider a multi-tone multi-antenna WPT system which has M transmit antennas, one receive antenna, and N tones at frequencies ω_1, ω_2,..., ω_N. The waveform sent by the mth transmit antenna can therefore be expressed as

$$x_m(t) = \Re\left\{\sum_{n=1}^{N} s_{m,n} e^{j\omega_n t}\right\}, \tag{1}$$

where $s_{m,n}$ denotes a weight (complex valued) representing the phase and magnitude for the nth tone at the mth transmit antenna. In addition, we define $\mathbf{s}_n = [s_{1,n}, s_{2,n}, \ldots, s_{M,n}]^T$ to represent the beamforming at the nth tone and we define $\mathbf{s} = [\mathbf{s}_1^T, \mathbf{s}_2^T, \ldots, \mathbf{s}_N^T]^T$ to represent the waveform and beamforming. The transmitter should satisfy a power constraint that can be expressed as

$$\frac{1}{2}\|\mathbf{s}\|^2 \le P, \tag{2}$$

where P represents the transmit power.

The multi-tone waveform sent by the multi-antenna transmitter propagates via a wireless channel. Accordingly, we can write the received waveform as

$$y(t) = \Re\left\{\sum_{n=1}^{N} \mathbf{h}_n \mathbf{s}_n e^{j\omega_n t}\right\}, \tag{3}$$

where $\mathbf{h}_n = [h_{1,n}, h_{2,n}, \ldots, h_{M,n}]$ with $h_{m,n}$ being the channel gain (complex valued) at the nth tone from the mth transmit antenna to the receive antenna. Due to the multipath fading channel, the received waveform $y(t)$ is different from the transmit waveform $x_m(t)$. Therefore, we need to consider the multipath fading channel when designing the optimal waveform and beamforming for WPT. From (3), the received RF power is given by

$$P_{\mathrm{RF}} = \frac{1}{2}\sum_{n=1}^{N} |\mathbf{h}_n \mathbf{s}_n|^2. \tag{4}$$

The received waveform is input into the rectifier to output dc power P_{DC}, which can be found by

$$P_{\mathrm{DC}} = P_{\mathrm{RF}}\eta\left(y(t)\right) = P_{\mathrm{DC}}\left(\mathbf{h}_1, \mathbf{h}_2, \ldots, \mathbf{h}_N, \mathbf{s}\right), \tag{5}$$

where $\eta(y(t))$ denotes the RF-to-dc efficiency given the input waveform $y(t)$. From (3) and (4), the output dc power

depends on the wireless channel gains $\mathbf{h}_n$ $\forall n$ and the waveform and beamforming weight vector $\mathbf{s}$, denoted as $P_{\mathrm{DC}}(\mathbf{h}_1, \mathbf{h}_2, \ldots, \mathbf{h}_N, \mathbf{s})$.

Assuming the CSI, i.e. the wireless channel gains $\mathbf{h}_n \forall n$, is known at the transmitter, the waveform and beamforming weight vector $\mathbf{s}$ can be optimized to adapt to the channel for maximizing the output dc power, which can be written as

$$\max_{\mathbf{s}} \quad P_{\mathrm{DC}}\left(\mathbf{h}_1, \mathbf{h}_2, \ldots, \mathbf{h}_N, \mathbf{s}\right) \tag{6}$$

$$\text{s.t.} \quad \frac{1}{2}\left\|\mathbf{s}\right\|^2 \leq P. \tag{7}$$

In the next subsections, we provide two strategies for designing adaptive waveform and beamforming for maximizing output dc power.

B. SCALED MATCHED FILTER

Scaled Matched Filter (SMF) is a strategy that can optimize the waveform and beamforming with a low complexity [48]. Using SMF, the beamforming weight vector $\mathbf{s}_n$ can be expressed as

$$\mathbf{s}_n = c\left\|\mathbf{h}_n\right\|^{\beta} \frac{\mathbf{h}_n^H}{\left\|\mathbf{h}_n\right\|}, \ \forall n, \tag{8}$$

where $\beta \geq 1$ is a parameter controlling the magnitude (l_2-norm) of $\mathbf{s}_n$ and c is a constant given by

$$c = \sqrt{\frac{2P}{\sum_{n=1}^{N}\left\|\mathbf{h}_n\right\|^{2\beta}}}, \tag{9}$$

so that the transmit power constraint can be satisfied. The SMF strategy only depends on the single parameter β. We set $\beta = 3$ in this work. In [48], it has been shown through simulation that the SMF strategy with $\beta = 3$ can provide performance which is close to the performance of optimal waveform and beamforming design proposed in [46] while its computational complexity is much lower.

Although the SMF has good performance and low computational complexity, it requires that the transmitter has the knowledge of CSI, i.e. $\mathbf{h}_n$ $\forall n$. It is challenging to acquire the CSI at the transmitter of WPT system since it needs channel estimation which increases the power consumption and circuit complexity. To overcome this challenge, in the next subsection, we provide another waveform and beamforming design strategy based on limited feedback.

C. LIMITED FEEDBACK

Consider a codebook consisting of K codewords, denoted as $\mathbf{s}^{(1)}$, $\mathbf{s}^{(2)}$,..., $\mathbf{s}^{(K)}$, with each codeword representing a particular waveform and beamforming weight vector. The basic idea of limited feedback strategy is to select the optimal codeword in the codebook for maximizing the output dc power. Specifically, the transmitter transfers wireless power to the receiver frame by frame to periodically adapt to the wireless channel. The frame period is designed to be shorter than the channel coherence time to ensure that the wireless channel gains $\mathbf{h}_n$ $\forall n$ are constant during one frame. There are training phase and WPT phase in each frame as shown in Fig. 1. Specifically, the training phase is designed to select the optimal codeword, i.e. the optimal waveform and beamforming, while the WPT phase is designed to transfer wireless power using the optimal waveform as well as beamforming. During the training phase, the transmitter sequentially chooses the K codewords as its waveform and beamforming to transfer wireless power while the receiver measures the output dc power for each codeword at the same time. The output dc power for the kth codeword $\mathbf{s}^{(k)}$ is given by $P_{\mathrm{DC}}(\mathbf{h}_1, \mathbf{h}_2, \ldots, \mathbf{h}_N, \mathbf{s}^{(k)})$. After measuring the output dc power level for the K codewords, the receiver can find the index of the optimal codeword maximizing the output dc power as

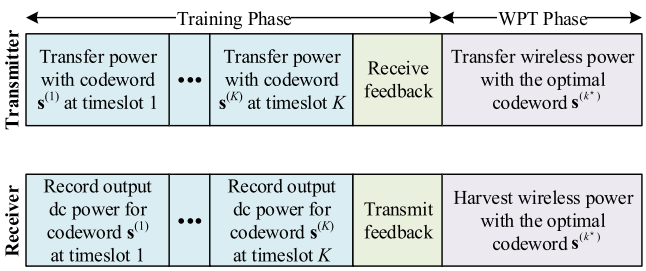

FIGURE 1. Time frame for the closed-loop WPT using limited feedback.

$$k^{\star} = \underset{k=1,\ldots,K}{\operatorname{argmax}} \ P_{\mathrm{DC}}\left(\mathbf{h}_1, \mathbf{h}_2, \ldots, \mathbf{h}_N, \mathbf{s}^{(k)}\right). \tag{10}$$

Then, the receiver feeds back the index of the optimal codeword $k^{\star}$ to the transmitter. Since there are K codewords in the codebook, we only need to feed back $\lceil \log_2 K \rceil$ bits representing the optimal codeword index, where $\lceil \cdot \rceil$ is the ceiling function. Once the transmitter receives the feedback $k^{\star}$, it can use the optimal codeword $\mathbf{s}^{(k^{\star})}$ as its waveform and beamforming to efficiently transfer wireless power during the WPT phase.

In contrast with the SMF strategy, the limited feedback strategy can enhance the output dc power without requiring the knowledge of CSI, i.e. $\mathbf{h}_n$ $\forall n$. Due to such benefit, we focus on using the limited feedback strategy to implement our closed-loop WPT system in this work. The key of limited feedback strategy in WPT is the design of an efficient codebook, which should have diverse codewords to match different wireless channel gains. In this work, we design an efficient codebook by following the approach proposed in [49]. Such approach considers the statistics of the multipath fading channel and the rectifier nonlinearity and leverages the Generalized Lloyd' s Algorithm (GLA) [49]. The main concept of GLA is to alternatively optimize the set partition and the partition centroid (representing the codeword) for a given training set. Simulation results have shown that the codebook designed by the approach can provide high output dc power.

We illustrate a codebook with 4 codewords ($K = 4$) which is designed for 8-tone 4-antenna WPT systems using the approach [49] as follows. The waveforms sent by the first

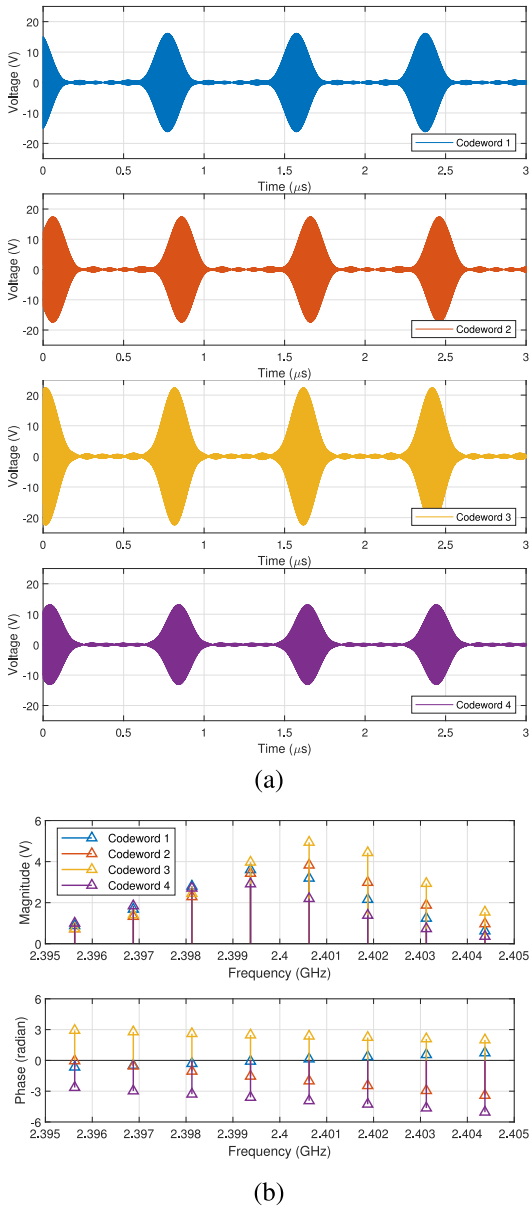

FIGURE 2. Waveforms sent by the first transmit antenna characterized by four different codewords in (a) time domain and (b) frequency domain.

transmit antenna characterized by different codewords in time and frequency domains are shown in Fig. 2. We can find that they are all eight-tone waveforms but have different magnitude and phase at each tone. Note that the total power for waveforms sent from all transmit antennas is constant while it is not constant for waveform sent by only one transmit antenna (e.g. codeword 3 is more powerful than codeword 4). The beamforming patterns at the first tone characterized by different codewords are shown in Fig. 3. We can find that the beamforming patterns characterized by different codewords point to different angles so that the codebook can cover a wide angle range. Overall, the waveform and beamforming changes with different codewords, showing that the codebook

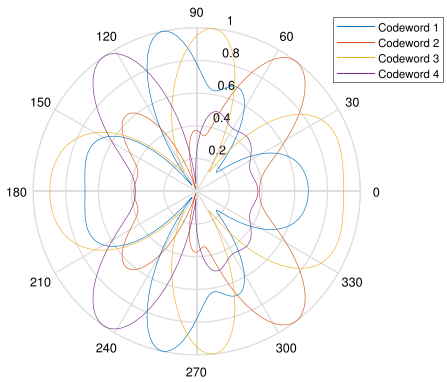

FIGURE 3. Beamforming patterns at the first tone characterized by four different codewords.

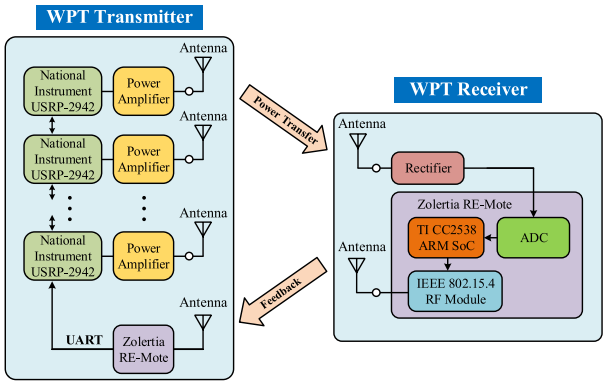

FIGURE 4. Diagram for the closed-loop WPT system using limited feedback.

can provide diverse waveform and beamforming to adapt to the channel for enhancing the output dc power. Besides, the output dc power can be increased by enlarging the codebook size K as there are more diverse codewords to select, however, at the expense of feeding back more bits.

III. CLOSED-LOOP WPT SYSTEM DESIGN

In this section, we provide a design for the closed-loop WPT system using limited feedback for adaptive waveform and beamforming, as illustrated in Fig. 4. We describe the transmitter design, receiver design, and flow chart as follows.

A. TRANSMITTER DESIGN

The transmitter is made up by two parts. The first part is made up by multiple antennas, power amplifiers, and SDR equipment, which is used to generate and radiate RF signals with waveform and beamforming characterized by different codewords. There are M transmit antennas in the first part and we consider three cases with $M = 1, 2$, and 4. All the antennas are identical 2.4-GHz monopole antennas which have omnidirectional radiation patterns. The radiation efficiency is 85% and the antenna gain is 3 dBi. We use M power amplifiers

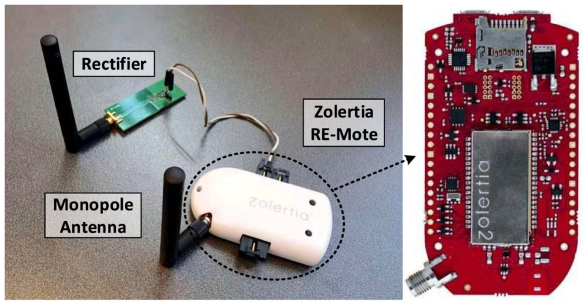

FIGURE 5. Photo for the receiver design and Zolertia RE-Mote.

(Mini-Circuits ZHL-16W-43-S+) to amplify the signal from the SDR equipment and each power amplifier is connected to a transmit antenna. The gain of power amplifier is 45 dB. We set the total transmit power as 33 dBm (2 W). The SDR equipment, National Instrument (NI) USRP-2942, is used to provide multi-tone signal having different phases and magnitudes at each tone. The multi-tone waveform has N tones and we consider four cases with $N = 1$, 2, 4, and 8. The N tones are uniformly distributed around 2.4 GHz with a bandwidth of $B = 10$ MHz. We use multiple USRP-2942 to generate multi-tone waveform for each transmit antenna so as to implement the adaptive waveform and beamforming.

The second part consists of a monopole antenna and a hardware development platform called Zolertia RE-Mote which is utilized to communicate with the receiver and acquire the optimal codeword fed back from the receiver. The Zolertia RE-Mote contains a 2.4-GHz RF interface under IEEE 802.15.4 standard and a system on chip from the Texas Instruments CC2538. A software platform called Contiki operating system is utilized to program the Zolertia. The Zolertia at the transmitter is utilized to send a message to the receiver (which also has a Zolertia) to start program and also to receive the index of the optimal codeword fed back from the receiver, through the RF interface operating at 2.42 GHz (that is different from the frequency of the multi-tone waveform for WPT). Therefore, the transmitter can transfer wireless power with the optimal waveform and beamforming so that the output dc power can be maximized.

B. RECEIVER DESIGN

As shown in Fig. 5, the receiver design is made up by two parts. The first part is a 2.4-GHz rectenna contains a monopole antenna and a single diode rectifier for harvesting wireless power. The antenna radiation efficiency is 85% and the antenna gain is 3 dBi. We reuse the single diode rectifier design in [54] for simplicity because the primary focus and contribution of this work is designing, prototyping, and experimenting a closed-loop WPT system using limited feedback technology, instead of designing a rectifier. The schematic and photo of the rectifier design are provided in Fig. 6. We adopt the Skyworks SMS7630 Schottky diode due to its low turn-on voltage that is good for low power rectification. Common

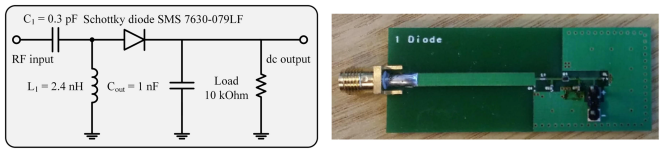

FIGURE 6. Schematic and photo for the rectifier design.

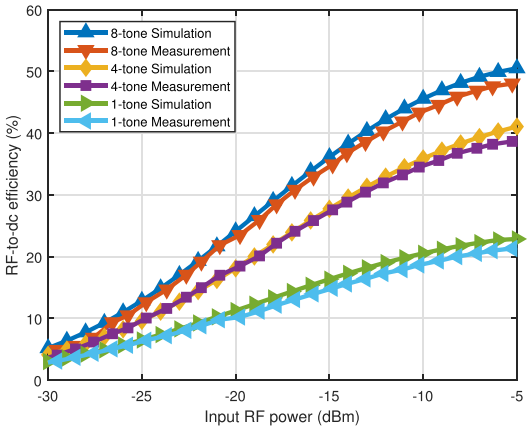

FIGURE 7. RF-to-dc efficiency of the rectifier design with 1-tone, 4-tone, and 8-tone waveforms. The 4-tone and 8-tone waveforms have 10 MHz bandwidth. The magnitude and phase of each tone in the 4-tone and 8-tone waveforms are identical.

materials including lumped elements and the FR-4 substrate with 1.6 mm thickness are used for rectifier design. The RF-to-dc efficiency with 1-tone, 4-tone, and 8-tone waveforms are shown in Fig. 7. The rectifier provides good RF-to-dc efficiency for multi-tone waveform while lower efficiency for 1-tone waveform. This is because it is difficult to find a load resistance simultaneously optimizing the RF-to-dc efficiency for the 1-tone and multi-tone waveforms. Since the proposed WPT system utilizes the multi-tone waveform, the load resistance is chosen as 10 kΩ to optimize the efficiency for multi-tone waveforms.

The second part contains a Zolertia RE-Mote with a monopole antenna, that is utilized to measure the output dc power and feed the index of the optimal codeword back to the transmitter. The Zolertia at the receiver measures the output dc power of rectenna by utilizing an analog-to-digital converter (ADC). The Zolertia searches all the measured output dc power to find the index of the optimal codeword and then utilizes the RF interface to feed the index back to the transmitter, so that the transmitter can transfer wireless power with the optimal waveform and beamforming.

C. FLOW CHART

Fig. 8 displays the flow chart for the proposed closed-loop WPT system using limited feedback. The transmitter transfers wireless power to the receiver frame by frame. As shown in Fig. 8, there are training phase and WPT phase in each frame.

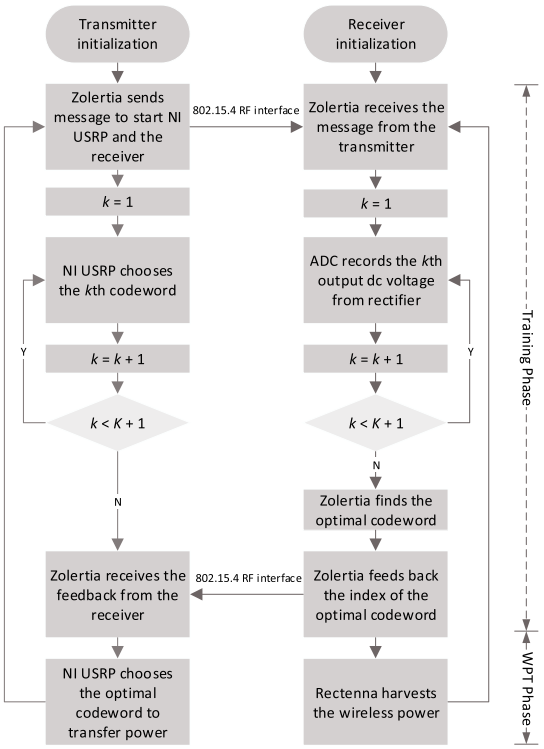

FIGURE 8. Flow chart of the closed-loop WPT system using limited feedback.

We utilize the training phase to find the optimal codeword, i.e. the optimal waveform and beamforming. At the transmitter, the Zolertia RE-Mote first transmits a message to the receiver and thus the receiver will start to work. It also transmits a message to the NI USRP-2942 through UART so that the NI USRP-2942 will start to work. The NI USRP-2942 sequentially chooses each codeword as its waveform and beamforming for power transfer. At the same time, the output dc voltage for each codeword will be measured by the receiver using the ADC in Zolertia RE-Mote. The time duration for each codeword is set as $T_s = 10$ ms and thus the training phase has time duration of KT_s. Once the output dc voltage for all codewords have been measured, the optimal codeword that maximizes the output dc voltage will be found. Generally, for a codebook having K codewords, the receiver only needs to feed back $\lceil \log_2 K \rceil$ bits representing the index of the optimal codeword. In this work, we consider codebooks having 2, 4, 8, 16, 32, and 64 codewords so that the receiver only needs to feed back 1, 2, 3, 4, 5, and 6 bits, respectively, to the transmitter using the RF interface. Then, the feedback index will be forwarded to NI USRP-2942 through UART so that the transmitter can choose the optimal codewords as its waveform and beamforming to transfer wireless power. Therefore, the closed-loop WPT system using limited feedback can improve the output dc power without requiring the knowledge of CSI.

We utilize the WPT phase to transfer wireless power using the optimal waveform and beamforming. The receiver keeps harvesting wireless power during this phase. Denoting the time duration for WPT phase as T_p, one frame has time duration of $T = KT_s + T_p = 2$ s. After the WPT phase of one frame, the proposed closed-loop WPT system will go to the training phase of the next frame to find another optimal codeword to adapt to the latest channel. Therefore, our proposed closed-loop WPT system can periodically (every 2 s) train the waveform and beamforming to adapt to the time-varying channel (e.g. when the transmitter or receiver moves) to maintain the maximum output dc power.

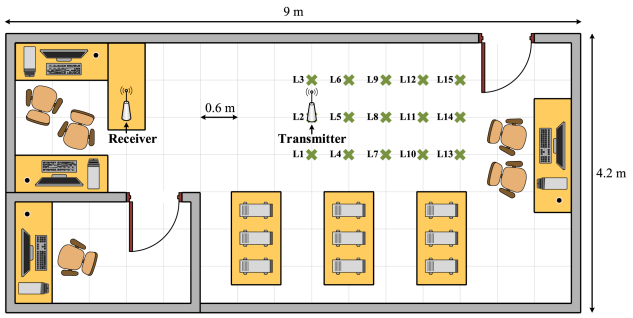

FIGURE 9. Illustration for the experiment in the indoor environment. The dimension of each box is 0.6 m×0.6 m.

Synchronization is an important issue which should be carefully handled when designing the closed-loop WPT system. At the beginning of training phase, the Zolertia at the transmitter will send a message to the NI USRP-2942 through UART and meanwhile send another message to the Zolertia at the receiver. The two messages will experience different delays. Hence, it is necessary to compensate the delays to achieve synchronization, so that the receiver can synchronously record the output dc voltage for each codeword and then find the optimal codeword. To that end, an oscilloscope is adopted to record the delays for sending messages to the NI USRP-2942 and the Zolertia at the receiver, respectively. Then, we program the NI USRP-2942 and the Zolertia at the receiver to wait for a certain time to compensate the measured delay for synchronization. Since the delay of message transmission is stable once the WPT system configuration is fixed, the synchronization achieved by measuring and compensating the delay are stable.

It is should be noted that the proposed closed-loop WPT system inherently captures the nonlinearity of rectifier since the selection of the codeword is made at the output dc power level (instead of RF power), hence capturing the influence of input signal on the rectification efficiency.

IV. CLOSED-LOOP WPT SYSTEM EXPERIMENT I

We prototype the proposed closed-loop WPT system using limited feedback and experiment the prototype in a 4.2 m × 9 m indoor environment which has facilities including tables and chairs as shown in Fig. 9 and thus has multipath fading. We fix the receiver location and place the transmitter at different locations denoted as L1-L15, so that we can evaluate

FIGURE 10. Photo for the closed-loop WPT system prototype and experiment in the indoor environment.

the closed-loop WPT system with different channels. Fig. 10 shows the photo for the closed-loop WPT system prototype and experiment in the indoor environment.

We consider using codebooks having 2, 4, 8, 16, 32, and 64 codewords in the closed-loop WPT system, which correspond to feeding back 1, 2, 3, 4, 5, and 6 bits. In addition, we also consider two benchmarks for comparison. The first benchmark is the SMF, which is a closed-loop strategy as shown in Section II. For the SMF strategy, the receiver performs complex channel estimation by using OFDM channel estimation and pilot transmission as shown in [52] and then feeds back the estimated CSI to the transmitter using cable. Such cable-based feedback is not practical but herein we just use it as a benchmark since it provides almost perfect CSI feedback (equivalently a large number of bits of feedback) to the transmitter. On the other hand, the second benchmark is the uniform power allocation (UP), which is an open-loop strategy allocating the same magnitude and phase to multiple tones and multiple antennas at the transmitter. Specifically, the complex weights for the UP strategy are

$$s_{m,n} = \sqrt{\frac{2P}{MN}}, \forall m,\ n, \tag{11}$$

which are independent of the CSI. Therefore, the UP strategy can be equivalently viewed as 0 bit of feedback.

A. OUTPUT DC VOLTAGE WAVEFORM

To demonstrate how the limited feedback strategy works, the output dc voltage waveform is measured by an oscilloscope. The measured output dc voltage waveform with 32 and 64 codewords in one frame are shown in Fig. 11. We can observe that there are training phase and WPT phase in one frame, confirming the proposed flow chart illustrated in Fig. 8. The output dc voltage varies overtime in the training phase, because the transmitter sequentially chooses each codeword as its waveform and beamforming to transfer wireless power. In addition, the output dc voltage does not change and maintains maximum in the WPT phase, because the transmitter adopts the optimal codeword (waveform and beamforming) to transfer power. In addition, using 64 codewords achieves a higher output dc voltage than using 32 codewords, which is however achieved at the expense of a longer training phase.

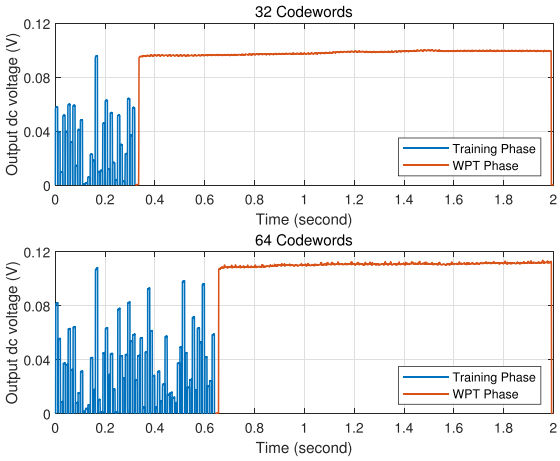

FIGURE 11. Output dc voltage waveform with 32 and 64 codewords in one frame.

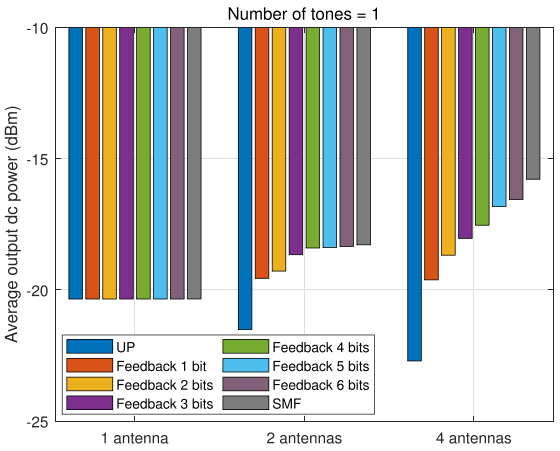

FIGURE 12. Average output dc power versus the number of transmit antennas with only 1 tone.

B. ADAPTIVE BEAMFORMING ONLY

First, we show the benefit of closed-loop WPT system with only adaptive beamforming using limited feedback. To that end, we consider the three strategies with only 1 tone and different numbers of transmit antennas, 1, 2, and 4. A multimeter is utilized to measure the output dc power at locations L1-L15 and the output dc power is averaged over the 15 locations. The average output dc power versus the transmit antenna number with only 1 tone is shown in Fig. 12. Following observations can be made.

1) The average output dc power can be enhanced by adopting more transmit antennas for the SMF and limited feedback strategies, showing the benefit of multi-antenna adaptive beamforming for output dc power enhancement. For the open-loop UP strategy, using more transmit antennas however reduces the output dc

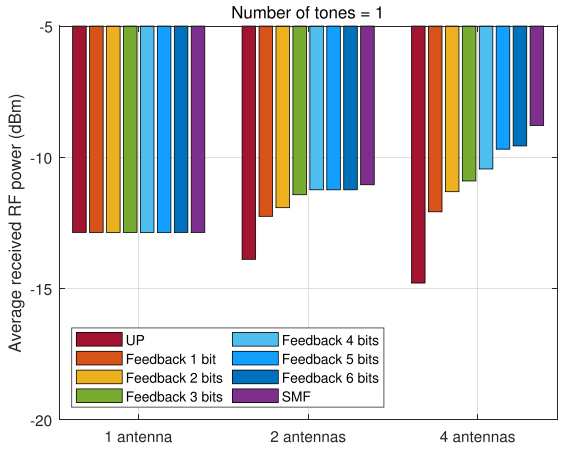

FIGURE 13. Average received RF power versus the number of transmit antennas with only 1 tone.

power. The reason is that the beam of multiple antennas using the UP strategy has fixed direction and narrow beamwidth, which leads to beam misalignment between the transmitter and receiver and reduces the output dc power.

2) The average output dc power for the closed-loop SMF and limited feedback strategies are higher than that for the open-loop strategy UP, showing the benefit of using closed-loop strategies to adapt beamforming to the wireless multipath fading channels.
3) The average output dc power for the limited feedback strategy enhances with the number of feedback bits. In other words, using more codewords can enhance the output dc power. Particularly, when the codebook has enough diverse codewords, the limited feedback strategy can achieve a similar performance to the SMF strategy while having the benefit that it does not require knowing the CSI.

Overall, we have shown that using adaptive beamforming with limited feedback is able to enhance the output dc power.

In addition, we provide the average received RF power[1] versus the transmit antenna number with only 1 tone in the Fig. 13. Following observations can be made. 1) The average received RF power can be enhanced by using more antennas for the SMF and limited feedback strategies, showing that using adaptive beamforming technology can effective enhance the average received RF power. 2) The closed-loop strategies achieves higher average received RF power than the open-loop strategy. 3) The average received RF power for the limited feedback strategy increases with the number of feedback bits, showing that using more diverse codewords can increase the average received RF power.

C. ADAPTIVE WAVEFORM ONLY

Next, we show the benefit of closed-loop WPT system with only adaptive waveform using limited feedback. To that end, we consider the three strategies with only 1 transmit antenna and different numbers of tones, 1, 2, 4, and 8. The output dc power at locations L1-L15 are measured and then averaged. The average output dc power versus the number of tones with only 1 transmit antenna is shown in Fig. 14(a). Following observations can be made.

1) The average output dc power can be enhanced by adopting more tones for the three strategies, showing the benefit of using multi-tone waveform in WPT for output dc power enhancement.
2) The output dc power for the closed-loop SMF and limited feedback strategies with more than 3 feedback bits are higher than that for the open-loop strategy UP, showing the benefit of using closed-loop strategies to adapt waveform to the wireless multipath fading channels.
3) The average output dc power for the limited feedback strategy can be enhanced by using more feedback bits, or more codewords, which is same as the adaptive beamforming only case. When the codebook has enough diverse codewords, the limited feedback strategy has a similar performance to the SMF strategy.

Overall, we have shown that using adaptive waveform with limited feedback is able to enhance the output dc power.

D. ADAPTIVE WAVEFORM AND BEAMFORMING

Finally, we show the benefit of joint adaptive waveform and beamforming using limited feedback. We consider the three strategies with $M = 2, 4$ transmit antennas and $N = 1, 2, 4, 8$ tones. The output dc power at L1-L15 are measured and averaged. The average output dc power versus tone number with different transmit antenna number is shown in Fig. 14. Following observations can be made.

1) Comparing the 8-tone cases and 1-tone cases in Fig. 14(b) and (c), it can be seen that the output dc power using the joint adaptive waveform and beamforming is higher than that using the adaptive beamforming only.
2) Comparing the 1-antenna case in Fig. 14(a) and the 2/4-antenna cases in Fig. 14(b) and (c), it can be seen that the output dc power using the joint adaptive waveform and beamforming is higher than the adaptive waveform only.
3) The output dc power for the closed-loop SMF and limited feedback strategies with more than 1 feedback bit are higher than that for the open-loop strategy UP, showing the benefit of using closed-loop strategies.
4) The average output dc power for the limited feedback strategy can be increased by using more feedback bits, or more codewords. When the codebook has enough

[1]For the proposed closed-loop WPT system, it is difficult to measure the received RF power since there is no interface at the rectenna to measure the received RF power. As a compromise, we can only compute the received RF power from the measured dc power as the RF-to-dc efficiency for 1-tone waveform is known. However, this method can be only used for 1-tone waveform because we cannot measure the received multi-tone waveform and the corresponding RF-to-dc efficiency is unknown.

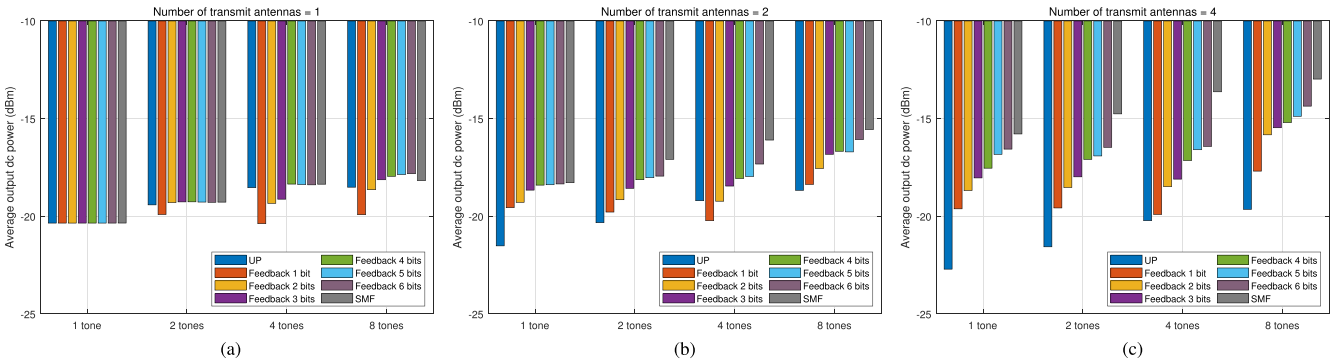

FIGURE 14. Average output dc power versus the number of tones with (a) only 1 transmit antenna, (b) 2 transmit antennas, and (c) 4 transmit antennas.

diverse codewords, the limited feedback strategy has a similar performance to the SMF strategy.

To show the benefit of the closed-loop WPT system using limit feedback, we further show the output dc power and end-to-end WPT efficiency for i) the conventional 1-tone 1-antenna WPT system, ii) the proposed 8-tone 4-antenna closed-loop WPT system with feeding back 6 bits, and iii) the benchmark 8-tone 4-antenna closed-loop WPT system using SMF at different locations in Fig. 15(a) and (b) respectively. The end-to-end WPT efficiency is defined as the ratio of output dc power and transmit RF power. Compared with the conventional 1-tone 1-antenna WPT system, the proposed closed-loop WPT system using limit feedback is able to enhance the output dc power by 2.2-14.7 dB and significantly increase the end-to-end WPT efficiency. For example, the end-to-end WPT efficiency can be increased from 4.3×10^{-7} to 1.3×10^{-5} at location 4 and from 9.7×10^{-6} to 5.8×10^{-5} at location 8. These demonstrates the benefit of our proposed WPT system. Besides, the limited feedback strategy has a similar output dc power and end-to-end WPT efficiency to that of the SMF strategy while having the benefit that it does not require knowing the CSI.

Overall, we have shown that the proposed closed-loop WPT system can boost the output dc power and end-to-end WPT efficiency without requiring the knowledge of CSI.

E. SELECTION OF NUMBER OF FEEDBACK BITS

Increasing the number of feedback bits will increase the output dc power in the WPT phase, but will also increase the complexity of the training phase, which leads to a longer training phase and a shorter WPT phase. To achieve the best trade-off between complexity and performance, we consider selecting the number of feedback bits to maximize the dc energy harvested in the WPT phase in one frame, which can be formulated as

$$b^{\star} = \underset{b=1,2,\ldots}{\operatorname{argmax}} \left(T - 2^{b} T_s\right) P_{\text{out}}^{\text{WPT}}(b) \tag{12}$$

where b denotes the number of feedback bits and $P_{\text{out}}^{\text{WPT}}(b)$ is the output dc power in the WPT phase given the number of feedback bits. With the setting $T = 2$ s and $T_s = 10$ ms,

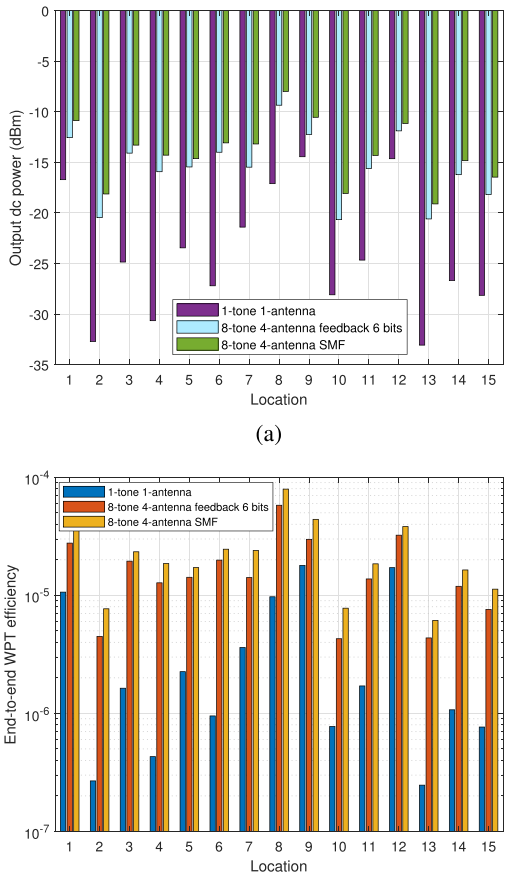

FIGURE 15. (a) Output dc power and (b) end-to-end WPT efficiency for the 1-tone 1-antenna WPT system, the proposed 8-tone 4-antenna closed-loop WPT system with feeding back 6 bits, and the 8-tone 4-antenna closed-loop WPT system using SMF at different locations.

the harvested dc energy in the WPT phase in one frame for 8-tone 4-antenna configuration is 33.7, 51.2, 54.5, 55.5, 54.6, and 49.8 μJ for 1, 2, 3, 4, 5, 6 feedback bits, respectively, so that we should select 4 feedback bits to achieve the best trade-off. In addition, if we increase T to 4 s, the impact

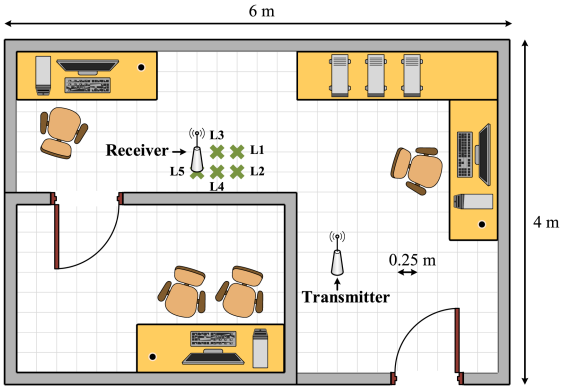

FIGURE 16. Illustration for the experiment in the indoor environment where the transmitter is at a corner. The dimension of each box is 0.25 m×0.25 m.

of training phase complexity will be reduced and we should select 6 feedback bits.

F. POWER BUDGET ANALYSIS

To evaluate the dc energy which is consumed by the Zolertia RE-Mote for limited feedback and the available harvested dc energy, a power budget analysis is detailed as follows.

First, the dc energy which is consumed by the Zolertia RE-Mote is estimated. As all the Zolertia RE-Mote modules are integrated, measuring the power consumption for each module is difficult. Hence, we can only refer to the datasheet provided by the vendor to estimate the power consumption. The system on chip CC2538 in the Zolertia RE-Mote works with low power consumption of $P_{\text{SoC}} = 2.6\ \mu\text{W}$, so that the consumed dc energy in one frame is $E_{\text{SoC}} = TP_{\text{SoC}} = 5.2\ \mu\text{J}$. Besides, some dc energy is consumed by the IEEE 802.15.4 RF interface to transmit a feedback which has data size of 1 byte. For the 802.15.4 RF interface, the power consumption is $P_{\text{RF}} = 48$ mW and the data rate is 250 kbps. Hence, in one frame the RF interface will work for $T_{\text{RF}} = 8$ bits/250 kbps $= 32\ \mu\text{s}$ and the corresponding consumed dc energy is $E_{\text{RF}} = T_{\text{RF}}P_{\text{RF}} = 1.54\ \mu\text{J}$. Therefore, the Zolertia RE-Mote in total consumes $E_{\text{ZoI}} = E_{\text{SoC}} + E_{\text{RF}} = 6.74\ \mu\text{J}$ in one frame.

Next, the available harvested dc energy is estimated. The rectenna can harvest dc energy in training phase (where the output dc power changes with time) and WPT phase (where the output dc power maintains maximum). For simplicity, we only count the dc energy harvested in the WPT phase. Consider the 8-tone 4-antenna configuration with 6 bits feedback. The output dc power is $P_{\text{out}}^{\text{WPT}} = 36.6\ \mu\text{W}$ during the WPT phase ($T_p = T - KT_s = 1.36$ s). Hence, the available harvested dc energy is $E_{\text{DC}} = T_p P_{\text{out}}^{\text{WPT}} = 49.8\ \mu\text{J}$ in one frame.

Lastly, the net available harvested dc energy can be estimated, that is $E_{\text{net}} = E_{\text{DC}} - E_{\text{ZoI}} = 43.1\ \mu\text{J}$ in one frame, so that the efficiency is $E_{\text{net}}/E_{\text{DC}} = 87\%$. Therefore, the dc energy consumed by the adaptive system is small compared with the harvested dc energy. In spite of the dc energy consumption, using the limited feedback strategy achieves a

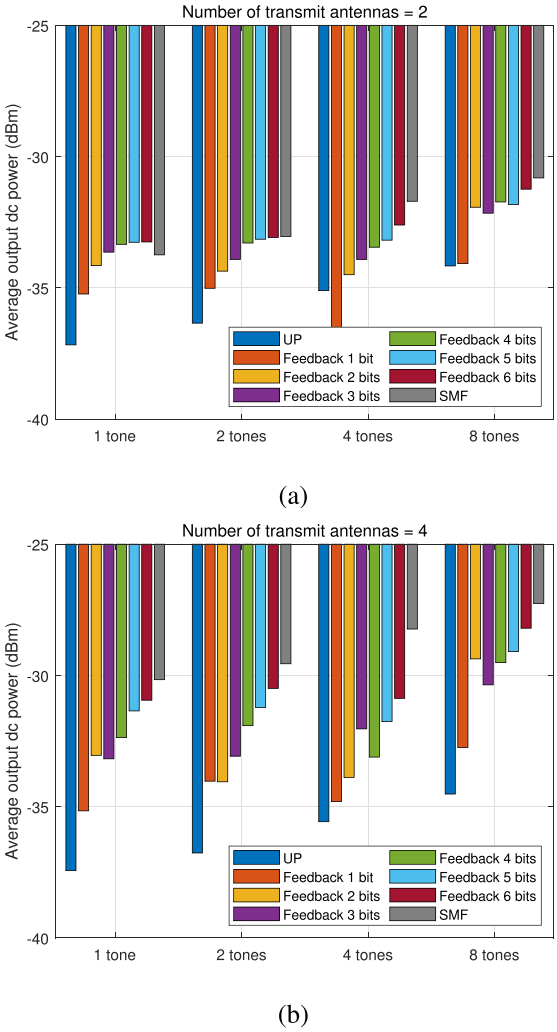

FIGURE 17. Average output dc power versus the number of tones with (a) 2 transmit antennas and (b) 4 transmit antennas. The transmitter is at a corner in the measurement environment.

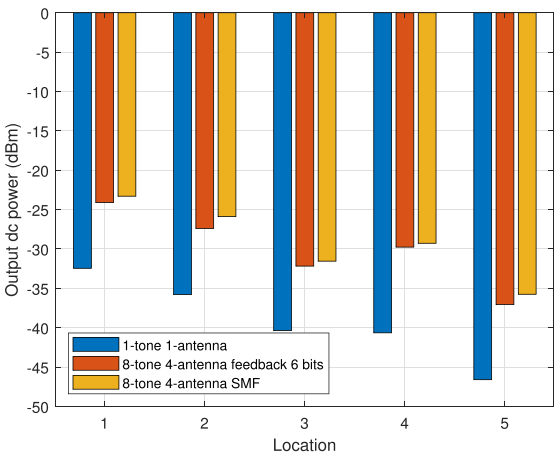

FIGURE 18. Output dc power with the receiver placed at different locations while the transmitter fixed at a corner in the measurement environment.

better performance than the conventional non-adaptive WPT system. In addition, the efficiency $E_{\text{net}}/E_{\text{DC}}$ can be further enhanced by increasing the frame time duration T, i.e. the portion of WPT phase in one frame. For example, if we set $T = 4$ s, we have that $E_{\text{net}}/E_{\text{DC}} = 90\%$. Since this work is aimed to demonstrate the benefit of utilizing adaptive waveform and beamforming with limited feedback in closed-loop WPT system, the architecture of receiver is simplified by using battery to energize the Zolertia, which will not influence the conclusion that utilizing adaptive waveform and beamforming with limited feedback is able to boost the output dc power. In practice, we can adopt a power management module to accumulate harvested energy as well as regulate the output voltage to an appropriate level to energize the Zolertia.

G. DISCUSSION ON MULTIPLE RECTIFIERS

We would like to highlight that our proposed closed-loop WPT system is also effective for multiple rectifiers. In the following, we consider two cases for multiple rectifiers.

For the first case of single user equipped with multiple rectennas, we can use dc combining to combine the different dc power output from multiple rectifiers, so we can select the optimal codeword to maximize the combined dc power.

For the second case of Q users each of which is equipped with a single rectenna, we can use time-division multiple access (TDMA). In the qth frame, we select the optimal codeword for maximizing the output dc power only for User q by following the same flow chart in Fig. 8, while the other $Q-1$ users will harvest the energy during the whole frame. By this way, we alternatively select the optimal codeword for each user at each frame.

Therefore, by using dc combining or TDMA, our proposed system is also effective for multiple rectifiers.

V. CLOSED-LOOP WPT SYSTEM EXPERIMENT II

To show that the proposed closed-loop WPT system is also effective when there is an obstacle between the transmitter and receiver, we also experiment it in a different 4 m $\times$ 6 m indoor environment, where we fix the transmitter at a corner and place the receiver at 5 different locations denoted as L1-L5 as illustrated in Fig. 16.

The output dc power at locations L1-L5 are measured and averaged. The measured average output dc power for the three strategies is shown in Fig. 17. From Fig. 17, we can make observations similar to the experiment without obstacle between the transmitter and receiver (Section IV), including: 1) the average output dc power can be enhanced by adopting more transmit antennas and more tones, 2) the average output dc power for the limited feedback strategy is higher than that for the open-loop UP strategy, 3) the limited feedback strategy has a similar performance to the SMF strategy when the codebook has enough codewords (more feedback bits).

We also provide the output dc power at the 5 locations for 1) conventional 1-tone 1 antenna WPT system, 2) the proposed 8-tone 4-antenna closed-loop WPT system with feeding back 6 bits, 3) the benchmark 8-tone 4-antenna WPT system using SMF in Fig. 18. From Fig. 18, we can make observations similar to the experiment without obstacle between the transmitter and receiver (Section IV), including 1) the proposed closed-loop WPT system achieves 8.3-10.8 dB higher output dc power than the conventional 1-tone 1-antenna WPT system, and 2) the proposed closed-loop WPT system achieves similar output dc power to the SMF strategy but does not require knowing the CSI.

Overall, we have shown that the proposed closed-loop WPT system can be also effectively used when there is an obstacle between the transmitter and the receiver.

VI. CONCLUSION

A closed-loop WPT system using limited feedback achieving enhanced output dc power is designed, prototyped, and experimented in this paper. To enhance the output dc power, we jointly exploit spatial and frequency domains by using adaptive multi-tone waveform and multi-antenna beamforming in WPT system to adapt the wireless channel.

A closed-loop architecture for WPT based on a codebook design and an over-the-air limited feedback utilizing an RF interface is proposed. With the limited feedback using codebook design, the channel estimation and accurate CSI can be avoided and more importantly the waveform and beamforming at the transmitter is optimized to adapt to the multipath fading channel in real time.

The proposed closed-loop WPT with adaptive waveform and beamforming using limited feedback is prototyped by a Software Defined Radio equipment and measured in a real indoor environment. A closed-loop WPT system using cable-feedback and an open-loop WPT system are measured as comparison benchmarks. The measurement results show that using closed-loop adaptive multi-tone waveform and multi-antenna beamforming can greatly enhance the output dc power. Compared with the conventional 1-tone 1-antenna WPT system, the proposed closed-loop WPT system using limited feedback is able to enhance the output dc power by up to 14.7 dB. Besides, the proposed closed-loop WPT system using limited feedback can achieve performance similar to the closed-loop WPT system using cable-feedback, while it is more practical and beneficial since it does not require any computationally complex and energy consuming channel estimation implementation at the receiver and does not rely on knowing the CSI accurately at the transmitter.

REFERENCES

[1] Z. Popovic, "Cut the cord: Low-power far-field wireless powering," *IEEE Microw. Mag.*, vol. 14, no. 2, pp. 55–62, Mar./Apr. 2013.

[2] C. Song, P. Lu, and S. Shen, "Highly efficient omnidirectional integrated multi-band wireless energy harvesters for compact sensor nodes of internet-of-things," *IEEE Trans. Ind. Electron.*, vol. 68, no. 9, pp. 8128–8140, Sep. 2021.

[3] S. Shen, C. Y. Chiu, and R. D. Murch, "A dual-port triple-band L-probe microstrip patch rectenna for ambient RF energy harvesting," *IEEE Antennas Wireless Propag. Lett.*, vol. 16, pp. 3071–3074, 2017.

[4] V. Palazzi et al., "A novel ultra-lightweight multiband rectenna on paper for RF energy harvesting in the next generation LTE bands," *IEEE Trans. Microw. Theory Techn.*, vol. 66, no. 1, pp. 366–379, Jan. 2018.

[5] S. Shen, Y. Zhang, C. Chiu, and R. Murch, "A triple-band high-gain multibeam ambient RF energy harvesting system utilizing hybrid combining," *IEEE Trans. Ind. Electron.*, vol. 67, no. 11, pp. 9215–9226, Nov. 2020.

[6] S. Shen, C. Y. Chiu, and R. D. Murch, "Multiport pixel rectenna for ambient RF energy harvesting," *IEEE Trans. Antennas Propag.*, vol. 66, no. 2, pp. 644–656, Feb. 2018.

[7] Y. Hu, S. Sun, H. Xu, and H. Sun, "Grid-array rectenna with wide angle coverage for effectively harvesting RF energy of low power density," *IEEE Trans. Microw. Theory Techn.*, vol. 67, no. 1, pp. 402–413, Jan. 2019.

[8] E. Vandelle, D. H. N. Bui, T.-P. Vuong, G. Ardila, K. Wu, and S. Hemour, "Harvesting ambient RF energy efficiently with optimal angular coverage," *IEEE Trans. Antennas Propag.*, vol. 67, no. 3, pp. 1862–1873, Mar. 2019.

[9] S. Shen, Y. Zhang, C.-Y. Chiu, and R. Murch, "An ambient RF energy harvesting system where the number of antenna ports is dependent on frequency," *IEEE Trans. Microw. Theory Techn.*, vol. 67, no. 9, pp. 3821–3832, Sep. 2019.

[10] S. Shen, Y. Zhang, C.-Y. Chiu, and R. Murch, "Directional multiport ambient RF energy-harvesting system for the Internet of Things," *IEEE Internet Things J.*, vol. 8, no. 7, pp. 5850–5865, Apr. 2021.

[11] W. Lin and R. W. Ziolkowski, "Electrically small Huygens CP rectenna with a driven loop element maximizes its wireless power transfer efficiency," *IEEE Trans. Antennas Propag.*, vol. 68, no. 1, pp. 540–545, Jan. 2020.

[12] A. Okba, A. Takacs, and H. Aubert, "Compact rectennas for ultra-low-power wireless transmission applications," *IEEE Trans. Microw. Theory Techn.*, vol. 67, no. 5, pp. 1697–1707, May 2019.

[13] L. Li, X. Zhang, C. Song, W. Zhang, T. Jia, and Y. Huang, "Compact dual-band, wide-angle, polarization-angle-independent rectifying metasurface for ambient energy harvesting and wireless power transfer," *IEEE Trans. Microw. Theory Techn.*, vol. 69, no. 3, pp. 1518–1528, Mar. 2021.

[14] M. A. Aldhaeebi and T. S. Almoneef, "Highly efficient planar metasurface rectenna," *IEEE Access*, vol. 8, pp. 214019–214029, 2020.

[15] T. S. Almoneef, F. Erkmen, M. A. Alotaibi, and O. M. Ramahi, "A new approach to microwave rectennas using tightly coupled antennas," *IEEE Trans. Antennas Propag.*, vol. 66, no. 4, pp. 1714–1724, Apr. 2018.

[16] J. A. Estrada et al., "RF-harvesting tightly coupled rectenna array tee-shirt with greater than octave bandwidth," *IEEE Trans. Microw. Theory Techn.*, vol. 68, no. 9, pp. 3908–3919, Sep. 2020.

[17] M. Huang et al., "Single- and dual-band RF rectifiers with extended input power range using automatic impedance transforming," *IEEE Trans. Microw. Theory Techn.*, vol. 67, no. 5, pp. 1974–1984, May 2019.

[18] J. Kimionis, A. Collado, M. M. Tentzeris, and A. Georgiadis, "Octave and decade printed UWB rectifiers based on nonuniform transmission lines for energy harvesting," *IEEE Trans. Microw. Theory Techn.*, vol. 65, no. 11, pp. 4326–4334, Nov. 2017.

[19] S. Fan et al., "A 2.45-GHz rectifier-booster regulator with impedance matching converters for wireless energy harvesting," *IEEE Trans. Microw. Theory Techn.*, vol. 67, no. 9, pp. 3833–3843, Sep. 2019.

[20] S. N. Daskalakis, A. Georgiadis, G. Goussetis, and M. M. Tentzeris, "A rectifier circuit insensitive to the angle of incidence of incoming waves based on a Wilkinson power combiner," *IEEE Trans. Microw. Theory Techn.*, vol. 67, no. 7, pp. 3210–3218, Jul. 2019.

[21] F. Zhao, D. Inserra, G. Gao, Y. Huang, J. Li, and G. Wen, "High-efficiency microwave rectifier with coupled transmission line for low-power energy harvesting and wireless power transmission," *IEEE Trans. Microw. Theory Techn.*, vol. 69, no. 1, pp. 916–925, Jan. 2021.

[22] S. A. Rotenberg, S. K. Podilchak, P. D. H. Re, C. Mateo-Segura, G. Goussetis, and J. Lee, "Efficient rectifier for wireless power transmission systems," *IEEE Trans. Microw. Theory Techn.*, vol. 68, no. 5, pp. 1921–1932, May 2020.

[23] Z. Zeng et al., "Design of sub-gigahertz reconfigurable RF energy harvester from −22 to 4 dBm with 99.8% peak MPPT power efficiency," *IEEE J. Solid-State Circuits*, vol. 54, no. 9, pp. 2601–2613, Sep. 2019.

[24] J. Bito, R. Bahr, J. G. Hester, S. A. Nauroze, A. Georgiadis, and M. M. Tentzeris, "A novel solar and electromagnetic energy harvesting system with a 3-D printed package for energy efficient Internet-of-Things wireless sensors," *IEEE Trans. Microw. Theory Techn.*, vol. 65, no. 5, pp. 1831–1842, May 2017.

[25] Y. Zhang, S. Shen, C. Y. Chiu, and R. Murch, "Hybrid RF-solar energy harvesting systems utilizing transparent multiport micromeshed antennas," *IEEE Trans. Microw. Theory Techn.*, vol. 67, no. 11, pp. 4534–4546, Nov. 2019.

[26] Y. Zeng, B. Clerckx, and R. Zhang, "Communications and signals design for wireless power transmission," *IEEE Trans. Commun.*, vol. 65, no. 5, pp. 2264–2290, May 2017.

[27] B. Clerckx, K. Huang, L. R. Varshney, S. Ulukus, and M.-S. Alouini, "Wireless power transfer for future networks: Signal processing, machine learning, computing, and sensing," *IEEE J. Sel. Topics Signal Process.*, vol. 15, no. 5, pp. 1060–1094, Aug. 2021.

[28] A. Boaventura, D. Belo, R. Fernandes, A. Collado, A. Georgiadis, and N. B. Carvalho, "Boosting the efficiency: Unconventional waveform design for efficient wireless power transfer," *IEEE Microw. Mag.*, vol. 16, no. 3, pp. 87–96, Apr. 2015.

[29] A. J. S. Boaventura, A. Collado, A. Georgiadis, and N. Borges Carvalho, "Spatial power combining of multi-sine signals for wireless power transmission applications," *IEEE Trans. Microw. Theory Techn.*, vol. 62, no. 4, pp. 1022–1030, Apr. 2014.

[30] F. Bolos, J. Blanco, A. Collado, and A. Georgiadis, "RF energy harvesting from multi-tone and digitally modulated signals," *IEEE Trans. Microw. Theory Techn.*, vol. 64, no. 6, pp. 1918–1927, Jun. 2016.

[31] A. J. S. Boaventura and N. B. Carvalho, "The design of a high-performance multisine RFID reader," *IEEE Trans. Microw. Theory Techn.*, vol. 65, no. 9, pp. 3389–3400, Sep. 2017.

[32] Z. Liu, Z. Zhong, and Y.-X. Guo, "*In vivo* high-efficiency wireless power transfer with multisine excitation," *IEEE Trans. Microw. Theory Techn.*, vol. 65, no. 9, pp. 3530–3540, Sep. 2017.

[33] A. Collado and A. Georgiadis, "Optimal waveforms for efficient wireless power transmission," *IEEE Microw. Wireless Compon. Lett.*, vol. 24, no. 5, pp. 354–356, May 2014.

[34] B. Clerckx, A. Costanzo, A. Georgiadis, and N. B. Carvalho, "Toward 1G mobile power networks: RF, signal, and system designs to make smart objects autonomous," *IEEE Microw. Mag.*, vol. 19, no. 6, pp. 69–82, Sept./Oct. 2018.

[35] S. Shen and B. Clerckx, "Beamforming optimization for MIMO wireless power transfer with nonlinear energy harvesting: RF combining versus DC combining," *IEEE Trans. Wireless Commun.*, vol. 20, no. 1, pp. 199–213, Jan. 2021.

[36] D. Belo, D. C. Ribeiro, P. Pinho, and N. B. Carvalho, "A selective, tracking, and power adaptive far-field wireless power transfer system," *IEEE Trans. Microw. Theory Techn.*, vol. 67, no. 9, pp. 3856–3866, Sep. 2019.

[37] D. Masotti, A. Costanzo, M. D. Prete, and V. Rizzoli, "Time-modulation of linear arrays for real-time reconfigurable wireless power transmission," *IEEE Trans. Microw. Theory Techn.*, vol. 64, no. 2, pp. 331–342, Feb. 2016.

[38] A. Costanzo and D. Masotti, "Smart solutions in smart spaces: Getting the most from far-field wireless power transfer," *IEEE Microw. Mag.*, vol. 17, no. 5, pp. 30–45, May 2016.

[39] B. Yang, X. Chen, J. Chu, T. Mitani, and N. Shinohara, "A 5.8-GHz phased array system using power-variable phase-controlled magnetrons for wireless power transfer," *IEEE Trans. Microw. Theory Techn.*, vol. 68, no. 11, pp. 4951–4959, Nov. 2020.

[40] P. S. Yedavalli, T. Riihonen, X. Wang, and J. M. Rabaey, "Far-field RF wireless power transfer with blind adaptive beamforming for Internet of Things devices," *IEEE Access*, vol. 5, pp. 1743–1752, 2017.

[41] K. W. Choi, L. Ginting, P. A. Rosyady, A. A. Aziz, and D. I. Kim, "Wireless-powered sensor networks: How to realize," *IEEE Trans. Wireless Commun.*, vol. 16, no. 1, pp. 221–234, Jan. 2017.

[42] S. Abeywickrama, T. Samarasinghe, C. K. Ho, and C. Yuen, "Wireless energy beamforming using received signal strength indicator feedback," *IEEE Trans. Signal Process.*, vol. 66, no. 1, pp. 224–235, Jan. 2018.

[43] H. Zhang, Y. Guo, S. Gao, and W. Wu, "Wireless power transfer antenna alignment using third harmonic," *IEEE Microw. Wireless Compon. Lett.*, vol. 28, no. 6, pp. 536–538, Jun. 2018.

[44] H. Zhang, Y. Guo, S. Gao, Z. Zhong, and W. Wu, "Exploiting third harmonic of differential charge pump for wireless power transfer antenna alignment," *IEEE Microw. Wireless Compon. Lett.*, vol. 29, no. 1, pp. 71–73, Jan. 2019.
[45] S. D. Joseph, Y. Huang, S. S. H. Hsu, A. Alieldin, and C. Song, "Second harmonic exploitation for high-efficiency wireless power transfer using duplexing rectenna," *IEEE Trans. Microw. Theory Techn.*, vol. 69, no. 1, pp. 482–494, Jan. 2021.
[46] B. Clerckx and E. Bayguzina, "Waveform design for wireless power transfer," *IEEE Trans. Signal Process.*, vol. 64, no. 23, pp. 6313–6328, Dec. 2016.
[47] Y. Huang and B. Clerckx, "Large-scale multiantenna multisine wireless power transfer," *IEEE Trans. Signal Process.*, vol. 65, no. 21, pp. 5812–5827, Nov. 2017.
[48] B. Clerckx and E. Bayguzina, "Low-complexity adaptive multisine waveform design for wireless power transfer," *IEEE Antennas Wireless Propag. Lett.*, vol. 16, pp. 2207–2210, 2017.
[49] Y. Huang and B. Clerckx, "Waveform design for wireless power transfer with limited feedback," *IEEE Trans. Wireless Commun.*, vol. 17, no. 1, pp. 415–429, Jan. 2018.
[50] S. Shen and B. Clerckx, "Joint waveform and beamforming optimization for MIMO wireless power transfer," *IEEE Trans. Commun.*, vol. 69, no. 8, pp. 5441–5455, Aug. 2021.
[51] J. Kim, B. Clerckx, and P. D. Mitcheson, "Prototyping and experimentation of a closed-loop wireless power transmission with channel acquisition and waveform optimization," in *Proc. IEEE Wireless Power Transfer Conf.*, 2017, pp. 1–4.
[52] J. Kim, B. Clerckx, and P. D. Mitcheson, "Signal and system design for wireless power transfer: Prototype, experiment and validation," *IEEE Trans. Wireless Commun.*, vol. 19, no. 11, pp. 7453–7469, Nov. 2020.
[53] J. Kim and B. Clerckx, "Range expansion for wireless power transfer using joint beamforming and waveform architecture: An experimental study in indoor environment," *IEEE Wireless Commun. Lett.*, vol. 10, no. 6, pp. 1237–1241, Jun. 2021.
[54] S. Shen, J. Kim, C. Song, and B. Clerckx, "Wireless power transfer with distributed antennas: System design, prototype, and experiments," *IEEE Trans. Ind. Electron.*, vol. 68, no. 11, pp. 10868–10878, Nov. 2021.

SHANPU SHEN (Member, IEEE) received the bachelor's degree in communication engineering from Nanjing University of Science and Technology, Nanjing, China, in 2013, and the Ph.D. degree in electronic and computer engineering from The Hong Kong University of Science and Technology (HKUST), Hong Kong, in 2017. He was a Visiting Ph.D. Student with the Microsystems Technology Laboratories, Massachusetts Institute of Technology, Cambridge, MA, USA, in 2016. He was a Postdoctoral Fellow with HKUST from 2017 to 2018, and he was a Postdoctoral Research Associate with the Communications and Signal Processing Group, Imperial College London, London, U.K., from 2018 to 2020. He is currently a Research Assistant Professor with HKUST. His research interests include RF energy harvesting, wireless power transfer, reconfigurable intelligent surface, Internet-of-Things, MIMO systems, and antenna design and optimization.

JUNGHOON KIM received the B.Sc. degree in electronic and electrical engineering from Hongik University, Seoul, South Korea, in 2008, and the M.Sc. degree in telecommunications from University College London, London, U.K., in 2015, and the Ph.D. degree in electrical and electronic engineering from Imperial College London, London, in 2020. From 2008 to 2014, he was with Mobile Communication Division, Samsung Electronics, Suwon, South Korea, as an R&D Engineer. From 2020 to 2022, he was a Postdoctoral Research Associate with the Department of Electrical and Electronic Engineering, Imperial College London. In 2022, he joined the Faculty with Korea Maritime and Ocean University, Busan, South Korea, where he is currently an Assistant Professor with the College of Ocean Science and Engineering. His research interests include RF energy harvesting, wireless information and power transfer, multiple-input and multiple-output systems, and Internet-of-Things.

BRUNO CLERCKX (Fellow, IEEE) received the M.Sc. and Ph.D. degrees in electrical engineering from the Université Catholique de Louvain, Belgium, and the Doctor of Science degree from Imperial College London, London, U.K. He is currently a Professor, the Head of the Wireless Communications and Signal Processing Laboratory, and the Deputy Head of the Communications and Signal Processing Group, within the Electrical and Electronic Engineering Department, Imperial College London, London, U.K. From 2006 to 2011, he was with Samsung Electronics, Suwon, South Korea, where he actively contributed to 4G (3GPP LTE/LTE-A and IEEE 802.16m). Since 2011, he has been with Imperial College London. From 2014 to 2016, he also was an Associate Professor with Korea University, Seoul, South Korea, and from 2021 to 2022, he was a Visiting Professor with Seoul National University, Seoul, South Korea. He also held various long or short-term visiting research appointments with Stanford University, Stanford, CA, USA, EURECOM, National University of Singapore, Singapore, The University of Hong Kong, Hong Kong, Princeton University, Princeton, NJ, USA, The University of Edinburgh, Edinburgh, U.K., The University of New South Wales, Kensington, NSW, Australia, and Tsinghua University, Beijing, China. He has authored two books: *MIMO Wireless Communications* and *MIMO Wireless Networks*, 250 peer-reviewed international research papers, and 150 standards contributions, and is the inventor of 80 issued or pending patents among which 15 have been adopted in the specifications of 4G standards and are used by billions of devices worldwide. His research interests include the general area of wireless communications and signal processing for wireless networks. He has been the TPC Member, the Symposium Chair, and TPC Chair of many symposia on communication theory, signal processing for communication and wireless communication for several leading international IEEE conferences. He was an Elected Member of the IEEE Signal Processing Society Signal Processing for Communications and Networking (SPCOM) Technical Committee. He was an Editor of IEEE TRANSACTIONS ON COMMUNICATIONS, IEEE TRANSACTIONS ON WIRELESS COMMUNICATIONS, and IEEE TRANSACTIONS ON SIGNAL PROCESSING. He has also been the (lead) Guest Editor for special issues of *EURASIP Journal on Wireless Communications and Networking*, IEEE ACCESS, IEEE JOURNAL ON SELECTED AREAS IN COMMUNICATIONS, IEEE JOURNAL OF SELECTED TOPICS IN SIGNAL PROCESSING, PROCEEDINGS OF THE IEEE, and IEEE OPEN JOURNAL OF THE COMMUNICATIONS SOCIETY. He was the Editor of the 3GPP LTE-Advanced Standard Technical Report on CoMP. He was the recipient of the prestigious Blondel Medal 2021 from France for exceptional work contributing to the progress of Science and Electrical and Electronic Industries, 2021 Adolphe Wetrems Prize in mathematical and physical sciences from Royal Academy of Belgium, multiple awards from Samsung, IEEE Best Student Paper Award, and EURASIP (European Association for Signal Processing) Best Paper Award 2022. He is a Fellow of IET and the IEEE Communications Society Distinguished Lecturer 2021–2022.